Journal of Applied Engineering Mathematics

Volume 8, December 2021

Design of Circular Piezoelectric Actuator for a Microfluidic Reconfigurable Radio Frequency Switch

Behzad Parsi, Tyler Stevens

Mechanical Engineering Department
Brigham Young University
Provo, Utah 84602
bparsi@byu.edu, trsteven@byu.edu

ABSTRACT

In this paper, for the first time, a novel alternative method is presented to reconfigure the RF signals by is using the microfluidic device. Nowadays, RF configuration can be achieved whether by microelectromechanical systems (MEMS) switches and MEMS capacitors, material loadings method, varactors, PIN diodes, or ferroelectric varactors. Although these methods have a great performance in terms of speed, cost, and size, they have several problems in terms of the power handling capability, and radiation efficiency and range of frequency tunability. In this research, we only focus on the designing of actuation method rather than designing the channel and RF switch. In this protype, we use cost-effective multi-sheet off-the-shelf piezoelectric material (e.g., PZT) as an actuator for valveless micropumps. For this purpose, we have derived analytic equations for expressing the natural frequency and mode shape of the actuator and membrane. In order to solve the governing equation, the Hankel transform in addition to Laplace transform will be utilized.

NOMENCLATURE

All parameters and calculations use SI units.
σ_1, and σ_2: Uniform constant tensions per unit length.
c_1, and c_2: Damping coefficient of the fluid surrounding the PZT, and diaphragm layer.
m_1, and m_2: Mass of PZT, and diaphragm layer.
k: Stiffness coefficient of the elastic foundation of Winkler type between PZT, and diaphragm layer.
r_0: Radius of the membranes.
w: Transverse motion of the membranes as function of membranes radius (r), and time (t).

INTRODUCTION

Reconfigurable radio frequency antennas and filters have drawn growing interest to enable compact and light weight multifunctional systems for wireless communications, sensor networks and biomedical imaging systems. The concept of microfluidics was introduced 40 years ago, with the advent of inkjet printing nozzle by IBM [1]. Later Gravesen et al. published a review paper about micropumping technologies and different actuating principles [2]. Afterwards many new fabrication technologies and in turn new micropump techniques have been developed, such as the positive displacement micropump by Cunneen et al. [3], the electro-osmotic micropump by Chen et al. [4], the pneumatic PDMS micropump by Jeong and Konishi [5], the piezoelectric micropump by S. Kaviani et al. [6], and the high pressure peristaltic micropump by Loth and Förster [7]. These are just some examples of the new fabrication methods in the microfluidics area, where the micropump design is highly dependent on specific applications. In general, being applied a voltage, a piezoelectric (e.g., PZT) layer bends inwards as a micropump [8]. This action can push fluid out of the chamber through the outlet valve. In the suction mode, when the voltage is removed, the PZT layer would back up to allow the fluid to enter the chamber. This reciprocating process would eventually cause the pumping action.
In this research, a PZT actuator which acts as micro pump will be design. The goal of this paper is not designing the microfluidics channel and RF switch.
This paper is organized as follows. In Section II, the governing analytic equations of the PZT layer with a bonding layer will be presented with their natural frequency and mode shape derived. In section III, the result will be presented and conclusion will be draw.

ANALYTIC MODELLING

The primary purpose of an optimized piezoelectric-layer actuator is to provide sufficient bending displacement in the transverse direction. As illustrated in Fig. 1, and 2, a piezoelectric layer, which might be physically implemented by multiple PZT sheets, is glued with the diaphragm layer. These two layers are assumed to connect each other by a massless and linear epoxy bonding layer.

The radius of the PZT layer and bonding layer is r_O, while their thicknesses are t_p and t_b, respectively.

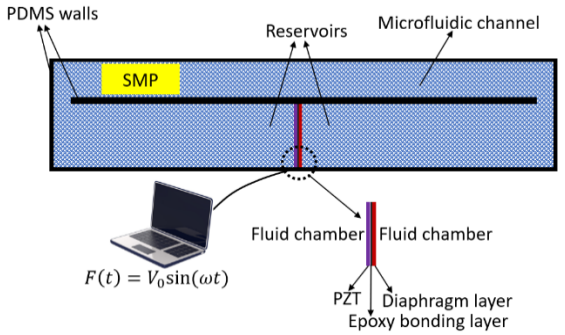

Fig. 1. Schematic view of the proposed microfluidic reconfigurable radio frequency switch.

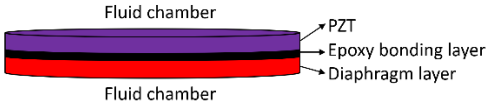

Fig. 2. Schematic view of piezoelectric actuator.

$$\sigma_1\left(\frac{\partial^2 w_1(r,t)}{\partial r^2}+\frac{1}{r}\frac{\partial w_1(r,t)}{\partial r}\right)=m_1\frac{\partial^2 w_1(r,t)}{\partial t^2}+k\big(w_1(r,t)-w_2(r,t)\big)+c_1\frac{\partial w_1(r,t)}{\partial t}+\alpha V_0\sin(\omega t) \quad (1)$$

$$\sigma_2\left(\frac{\partial^2 w_2(r,t)}{\partial r^2}+\frac{1}{r}\frac{\partial w_2(r,t)}{\partial r}\right)=m_2\frac{\partial^2 w_2(r,t)}{\partial t^2}-k\cdot\big(w_1(r,t)-w_2(r,t)\big)+c_2\frac{\partial w_2(r,t)}{\partial t} \quad (2)$$

where $\sigma_1$and σ_2 are the applied tension on the piezoelectric layer and diaphragm layer respectively, w_1 and w_2 are the displacement of the piezoelectric layer and diaphragm layer respectively, k is the stiffness coefficient of the epoxy layer, m_1 and m_2 are the mass per unit area of the piezoelectric layer and diaphragm layer respectively.

As a result, the boundary condition equations can be written as follows:

$$\begin{cases} w_1(r_o,t)=0, w_1(0,t)\neq\infty \\ w_2(r_o,t)=0, w_2(0,t)\neq\infty \end{cases} \quad (3)$$

Moreover, the PZT layer has no initial velocity:

$$\begin{cases} w_1(r,0)=0\,, \frac{\partial w_1}{\partial t}(r,0)=0 \\ w_2(r,0)=0\,, \frac{\partial w_2}{\partial t}(r,0)=0 \end{cases} \quad (4)$$

Hence, the governing equations are in polar coordinate, the Henkel transform will be performed. The differential operator, the Hankel transform and the inverse Hankel transform are defined as

$$Lw\equiv\frac{1}{r}\frac{\partial}{\partial r}\left(r\frac{\partial w}{\partial r}\right)=-\lambda^2 w \quad (5)$$

$$H_0\{w_i\}=\tilde{w}_i=\int_0^{r_0} w_i(r)J_0(\lambda_j r)\,r dr \quad (6)$$

$$H_0^{-1}\{\tilde{w}_i\}=w_i=\sum\tilde{w}_i\frac{J_0(\lambda_j r)}{\left\|J_0(\lambda_j r)\right\|^2} \quad (7)$$

where the eigen values λ_j $(j=n,or\ m)$ are positive roots of $J_0\left(\lambda_j r_0\right)=0$. The eigenfunctions and norms will be calculated as follow:

$$X_{1n}(r)=J_0\left(\lambda_n r\right) \quad (8)$$

$$X_{1m}(r)=J_0\left(\lambda_m r\right) \quad (9)$$

$$\left\|J_0\left(\lambda_n r\right)\right\|^2=\frac{r_0^2}{2}J_1^2\left(\lambda_n r_0\right) \quad (10)$$

$$\left\|J_0\left(\lambda_m r\right)\right\|^2=\frac{r_0^2}{2}J_1^2\left(\lambda_m r_0\right) \quad (11)$$

By applying Hankel transform the governing equations will be rewritten as follows:

$$-\sigma_1\lambda_n^2\tilde{w}_1=m_1\frac{\partial^2\tilde{w}_1}{\partial t^2}+k(\tilde{w}_1-\tilde{w}_2)+c_1\frac{\partial\tilde{w}_1}{\partial t}+\int_0^{r_0}\alpha V_0\sin(\omega t)J_0(\lambda_n r)\,r dr \quad (12)$$

$$-\sigma_1\lambda_m^2\tilde{w}_2=m_2\frac{\partial^2\tilde{w}_2}{\partial t^2}-k(\tilde{w}_1-\tilde{w}_2)+c_2\frac{\partial\tilde{w}_2}{\partial t} \quad (13)$$

Now, the Laplace transform in the time variable domain, $\widetilde{W}(s)=\int_0^\infty\tilde{w}(t)e^{-st}dt$, will be applied to the governing equation.

$$\widetilde{W}_1(s)(m_1s^2+c_1s+k+\sigma_1\lambda_n^2)-\widetilde{W}_2(s)k=-\mathcal{L}\{\sin(\omega t)\}\left(\frac{\alpha V_0}{\lambda_n}r_0J_1(\lambda_n r_0)\right) \quad (14)$$

$$\widetilde{W}_2(s)(m_2s^2+c_2s+k+\sigma_2\lambda_m^2)-\widetilde{W}_1(s)k=0 \quad (15)$$

The equations 14 and 15 can be solved by inverse matrix technique, and then the inverse Laplace transform using the convolution theorem can be utilized as follow:

$$\begin{bmatrix} m_1 s^2 + c_1 s + k + \sigma_1 \lambda_n^2 & -k \\ -k & m_2 s^2 + c_2 s + k + \sigma_2 \lambda_m^2 \end{bmatrix} \begin{bmatrix} \widetilde{W}_1(s) \\ \widetilde{W}_2(s) \end{bmatrix} = \begin{bmatrix} -\mathcal{L}\{\sin(\omega t)\} \left(\frac{\alpha V_0}{\lambda_n} r_0 J_1(\lambda_n r_0) \right) \\ 0 \end{bmatrix} \tag{16}$$

$$\widetilde{w}_1(t) = \mathcal{L}^{-1}\{\widetilde{W}_1(s)\},\ \widetilde{w}_2(t) = \mathcal{L}^{-1}\{\widetilde{W}_2(s)\} \tag{17}$$

Now, by applying the inverse Hankel transform, the final solution can be written as:

$$w_1(r,t) = \sum_{n=1}^{\infty} \widetilde{w}_1(t) \frac{J_0(\lambda_n r)}{\|J_0(\lambda_n r)\|^2} \tag{18}$$

$$w_2(r,t) = \sum_{m=1}^{\infty} \widetilde{w}_2(t) \frac{J_0(\lambda_m r)}{\|J_0(\lambda_m r)\|^2} \tag{19}$$

RESULTS AND DISCUSSION

Since the analytic equations, which show the relationship among the thickness of the piezoelectric layer, the thickness of the diaphragm layer, the radius of the layers, and the maximum deflection of the layers as discussed in Section II, are able to accurately estimate the natural frequency and system response. The material properties within the system are shown in table I and II, and the first and second natural frequency is represented in table III and, visually, in Fig. 3 a-d. Since, the pumping mode occurs only in first mode shape (3149 Hz), the frequency of input voltage must be tuned same as the natural frequency to get the maximum pumping performance.

TABLE I
THE OPTIMIZATION AND INPUT PARAMETERS OF THE SYSTEM.

	diaphragm layer thickness	piezoelectric layer thickness	Radius
Value	110 μm	92 μm	5 mm

TABLE II
MATERIAL PROPERTIES WITHIN THE SYSTEM.

Mechanical property	Diaphragm layer (silicon nitride)	Bonding layer (epoxy resin)	PZT (lead zirconate titanate)
Mass density	3290 (Kg/m^3)	2000 (Kg/m^3)	7500 (Kg/m^3)
Elastic modulus	310 (GPa)	5.17 (GPa)	9.5 (GPa)
Poisson's ratio	0.27	0.31	0.30

TABLE III
THE FIRST, SECOND NATURAL FREQUENCIES

Natural Frequency	(Hz)
1st	3149
2nd	4735

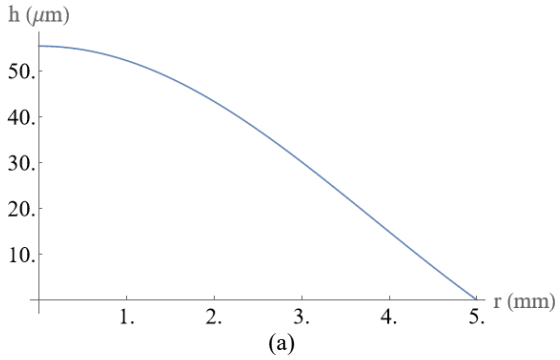

(a)

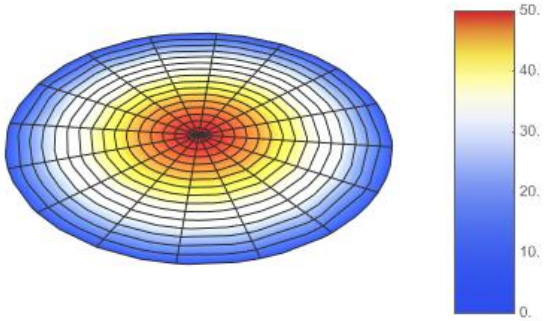

(b)

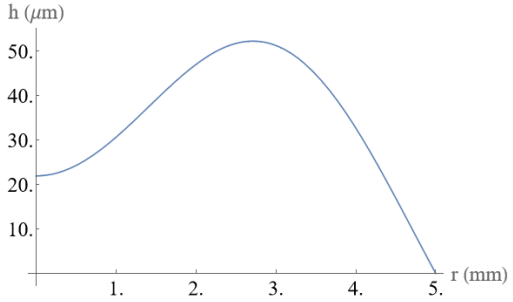

(c)

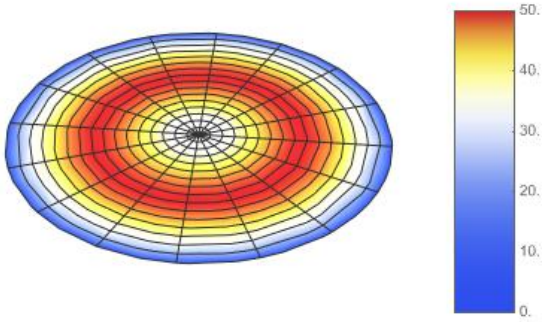

(d)

Fig. 3. The PZT layer, (a) The first mode shape, (b) The 3D model of the first mode shape, (c) The second mode shape, and (d) The 3D model of the second mode shape mode shape.

CONCLUSIONS

In this research, we proposed a new design approach to implement microfluidic RF devices within mm-wave band by considering motion dependent RF parasitic resulting from the in-plane motion of the metallized plates. In order to reach to this goal, we designed the circular PZT actuator. Which, to maximize the displacement of the pumped fluid, must operate at the natural frequency of the actuator. This, in turn, allows designers to efficiently estimate the maximum rate of pumped fluid, the system's natural frequencies and mode shapes of a new cylindrical configuration dimensions without depending on any expensive FEM simulations.

ACKNOWLEDGMENTS

The authors would like to thank Prof. Soloviev.

REFERENCES

[1] B. Parsi, L. Zhang and V. Masek, "Disposable Off-Chip Micro-Dispenser for Accurate Droplet Transportation," in *IEEE Sensors Journal*, vol. 19, no. 2, pp. 575-586, 15 Jan.15, 2019, doi: 10.1109/JSEN.2018.2878484.

[2] P. Gravesen, J. Branebjerg, and O. S. Jensen, "Microfluidics-a review," *Journal of Micromechanics and Microengineering,* vol. 3, no. 4, pp. 168–182, Jan. 1993.

[3] J. Cunneen, Y.-C. Lin, S. Caraffini, J. G. Boyd, P. J. Hesketh, S. M. Lunte, and G. S. Wilson, "A positive displacement micropump for microdialysis," *Mechatronics,* vol. 8, no. 5, pp. 561–583, 1998.

[4] Z. Chen, P. Wang, and H.-C. Chang, "An electro-osmotic micro-pump based on monolithic silica for micro-flow analyses and electro-sprays," *Analytical and Bioanalytical Chemistry,* vol. 382, no. 3, pp. 817–824, Jan. 2005.

[5] O. C. Jeong and S. Konishi, "Fabrication and drive test of pneumatic PDMS micropump," *Sensors and Actuators A: Physical,* vol. 135, no. 2, pp. 849–856, 2007.

[6] S. Kaviani, M. Bahrami, A. M. Esfahani, and B. Parsi, "A modeling and vibration analysis of a piezoelectric micro-pump diaphragm," *Comptes Rendus Mécanique,* vol. 342, no. 12, pp. 692–699, 2014.

[7] A. Loth and R. Forster, "Disposable high pressure peristaltic micropump for standalone and on-chip applications," in *2016 IEEE 11th Annual International Conference on Nano/Micro Engineered and Molecular Systems (NEMS)*, 2016.

[8] B. Parsi, L. Zhang and V. Masek, "Vibration analysis of a double circular PZT actuator for a valveless micropump", *Proc. CSME Int. Conf.*, pp. 27-30, May 2018.

